Peridynamic formulation of the mean stress and incubation time fracture criteria and its correspondence to the classical Griffith's approach

M.O. Ignatiev[1], Y.V. Petrov[1,2], N.A. Kazarinov[2,3], E. Oterkus[4]

[1]Saint Petersburg State University, Saint Petersburg, Russia

[2]Institute for Problems of Mechanical Engineering, Saint Petersburg, Russia

[3]Emperor Alexander I Saint Petersburg State Transport University, Saint Petersburg, Russia

[4]University of Strathclyde, Glasgow, United Kingdom

Abstract

Peridynamic formulations of the mean stress and incubation time fracture models are discussed in the paper. Contemporary fracture simulations using the peridynamic theory often rely on critical bond stretch fracture criterion which is known to operate similarly to energy-based fracture models. The energy-based fracture criteria – both in classical Griffith's and Irwin's form – are known to be powerful tools for fracture simulations and analysis. However, a number of experimentally observed dynamic fracture effects cannot be captured by these models, e.g. rate sensitivity of the material toughness. Thus, coupling of peridynamic approach with alternative stress-based fracture models would possibly broaden the peridynamics applicability. Here implementation technique of the aforementioned fracture model is discussed and its results for the case of a dynamically propagating crack with relatively low velocity due to quasistatic load appear to be in good agreement with the classical energy release rate approach.

Keywords: brittle fracture, peridynamics, Griffith's approach, fracture criterion, structural criterion, incubation time.

1. Introduction

Fracture mechanics as an independent science originates in the 20s of the last century, when A.A. Griffiths established the energy principle of crack propagation in an elastic body [1]. According to this principle, the total potential energy of a body containing a crack is a function of the crack length, and its movement is accompanied by a decrease in the elastic potential energy, which is spent on the formation of new crack surfaces, and the critical energy release rate per unit area γ is a material constant. Thus, according to the Griffith's concept the

This is a peer reviewed, accepted author manuscript of the following research article: Ignatiev, M. O., Petrov, Y. V., Kazarinov, N. A., & Oterkus, E. (2022). Peridynamic formulation of the mean stress and incubation time fracture criteria and its correspondence to the classical Griffith's approach. Continuum Mechanics and Thermodynamics. https://doi.org/10.1007/s00161-022-01159-8

infinitesimal crack elongation takes place, when sufficient amount of energy is provided for the formation of the new surfaces:

$$-\frac{d\Omega}{dl} \geq 2\gamma \quad (1).$$

In (1)$d\Omega$is an elastic strain energy increment and dl is a crack length increment. The criterion (1)yields remarkably accurate strength predictions for quasistatically loaded samples with cracks. However, limitations of (1) are also well-known, including its inability to work with angular notches without proper modifications [2]. Another widely used energy-based fracture criterion for a cracked body is Irwin's fracture condition which implies comparison of the current stress intensity factor (SIF) K_I with some ultimate SIF value K_{IC}, which is a material parameter:

$$K_I \geq K_{IC} \quad (2).$$

In (2) mode-I load is supposed, though similar conditions can also be written for the other loading modes. Criterion (2) works reliably for stationary cracks and quasistatic loads, but fails to predict crack initiation for intensive high-rate loads requiring introduction of new ultimate SIF value for each loading rate. The situation is even more complicated in case of moving cracks due to known lack of K-dominance for the fastpropagating cracks [3].

However, (2)is often modified to address dynamically propagating cracks. For example, the static ultimate SIF value is substituted by a $K_I(v)$ relation which decribes dependence of the current SIF on a crack velocity v. This relation is regarded as a material property and is supposed to be evaluated experimantally for each material. However, it was found that for some loads [4] and specimen types [5] this relation can be inconsistent and non-unique and thus the corresponding fracture model may yield erroneous results.

Alternative fracture criteria are able to resolve some of the mentioned problems. For example, the incubation time fracture criterion (ITFC) [6,7] is able to predict some fundamental dynamic fracture effects. This fracture model does not rely on the energy release rate or SIF concepts, but rather explicitly involve stress field values and thus help to evade the mentioned controversy. Peridynamic implementation of two stress-based fracture models (mean stress fracture model and ITFC) are discussed. Additionally, performance of these fracture models is compared to conventional critical bond stretch criterion (which in its turn correlates with energy release rate criterion [8]) for a quasistatic load case and relatively low crack propagation velocities. The studied regimes suppose that both models will provide similar results and thus the developed numerical scheme could be verified. Peridynamic models of ITFC already demonstrated some experimental phenomena of the dynamic fracture [9,10]. The computations

were performed using peridynamic software Peridigm [11] with additional procedures implementing the ITFC.

2. Peridynamics

In early 2000s a novel nonlocal solid mechanics theory was presented by Silling [12,13] and became a very powerful tool particularly for solving the problems of fracture mechanics. Nowadays it is a fast-developing field of science and many researchers have already made a decent contribution to the theory and its applications [14-16]. In this section, we briefly describe some basics of peridynamics.

Peridynamics is known to be a reformulation of the standard continuum theory. The solid body is simulated by a set of non-locally interacting particles. Each particle x has a family of neighbour particles $\mathcal{H}_x$ which influence its behavior. The subset $\mathcal{H}_x$ contains particles which are located in sphere of a specific radius (horizon) centered at x (Fig. 2). On the contrary, continuum theory deals with infinitely small elements interacting with each other only if they are in contact, i.e. there is a zero distance between them. It should be mentioned that the idea to account for non-local interactions inside the medium is far from being new or revolutionary, one can explore its roots and corresponding references in comprehensive works [17,18]. Moreover, concepts of smoothing and delocalization have naturally found their way into the numerical methods area and such methods as phase-field modelling [19], SPH [20] and many others are actively used by researchers and engineers to simulate fracture.

Nevertheless, if there is no non-local behaviour presented in the structure, for instance, discontinuity of the strain field in the region of the contact between stiff and compliant layers in the composite structure or singularity in the vicinity of the crack tip, then peridynamic approach converges to the classical one when a radius of the spherical region of influence approaches to zero, i.e. in this case peridynamics and classical approach are equal [21].

An equation of motion in the standard theory operates with the spatial derivatives of the continuum stress field which is defined as:

$$\rho(\mathbf{x})\ddot{\mathbf{u}}(\mathbf{x},\mathrm{t}) = \nabla\cdot\boldsymbol{\sigma}(\mathbf{x},\mathrm{t}) + \mathbf{b}(\mathbf{x},\mathrm{t}) \qquad (3),$$

where $\rho(\mathbf{x})$, $\ddot{\mathbf{u}}(\mathbf{x},\mathrm{t})$, $\mathbf{b}(\mathbf{x},\mathrm{t})$ are mass density, acceleration and body force density, respectively, $\boldsymbol{\sigma}(\mathbf{x},\mathrm{t})$ is a stress tensor; $\mathbf{x}$ and t are position vector in the reference configuration and time, respectively.

The peridynamics equation of motion is composed of integration of the non-local forces between the particles and can be written as:

$$\rho(\mathbf{x})\ddot{\mathbf{u}}(\mathbf{x},t)=\int_{\mathcal{H}_x}\left\{\underline{\mathbf{T}}[\mathbf{x},t]\langle\mathbf{x}'-\mathbf{x}\rangle-\underline{\mathbf{T}}[\mathbf{x}',t]\langle\mathbf{x}-\mathbf{x}'\rangle\right\}dV_{\mathbf{x}'}+\mathbf{b}(\mathbf{x},t) \quad (4),$$

where $\mathbf{x}'$ is the position vector of any neighbour of the particle $\mathbf{x}$ in its neighbourhood $\mathcal{H}_x$.A vector state $\underline{\mathbf{A}}$ maps the vectors into the vectors as well as the second-order tensor (difference between them is that vector state can be a nonlinear or discontinuous function and therefore it's something more general than a second-order tensor).$\underline{\mathbf{T}}=\underline{\widehat{\mathbf{T}}}(\underline{\mathbf{Y}})$is the force vector state function, which maps the deformation vector state $\underline{\mathbf{Y}}$into the force-vector state $\underline{\mathbf{T}}[\mathbf{x},t]$(in the angle brackets, $\langle\mathbf{x}'-\mathbf{x}\rangle$, we indicate the bond, that is, an interaction between two particles, which a force state operates on).

Deformation vector-state $\underline{\mathbf{Y}}[\mathbf{x},\mathrm{t}]\langle\boldsymbol{\xi}\rangle$(where $\boldsymbol{\xi}=\mathbf{x}'-\mathbf{x}$) can be defined as:

$$\underline{\mathbf{Y}}[\mathbf{x},\mathrm{t}]\langle\boldsymbol{\xi}\rangle=\mathbf{y}(\mathbf{x}+\boldsymbol{\xi},t)-\mathbf{y}(\mathbf{x},t) \quad (5),$$

where $\mathbf{y}(\mathbf{x},\mathrm{t})$ is the position of $\mathbf{x}$ at time t after deformation which is defined as:

$$\mathbf{y}(\mathbf{x},t)=\mathbf{x}+\mathbf{u}(\mathbf{x},t) \quad (6),$$

Where $\mathbf{u}(\mathbf{x},\mathrm{t})$ is the displacement field. Therefore,$\underline{\mathbf{Y}}[\mathbf{x},\mathrm{t}]\langle\boldsymbol{\xi}\rangle$ is the image of $\boldsymbol{\xi}$after deformation.

Transformation of the equation of motion mentioned above plays a crucial role for the fracture mechanics since the absence of the spatial derivatives allows to overcome the obstacles of the classical theory, such as discontinuities.

Thus, each of two interacting particles of the bond has its own force vector and in the general state-based peridynamics these vectors are not equal (instead of the bond-based approach, Fig. 1). If we assume that force vector remains parallel to the vector which connects $\mathbf{x}$ and $\mathbf{x}'$ in deformed configuration, then such approach is called an ordinary state based peridynamics, otherwise it is called a non-ordinary state based peridynamics. In this paper we will consider an ordinary state based linear peridynamic solid (LPS) material [13].

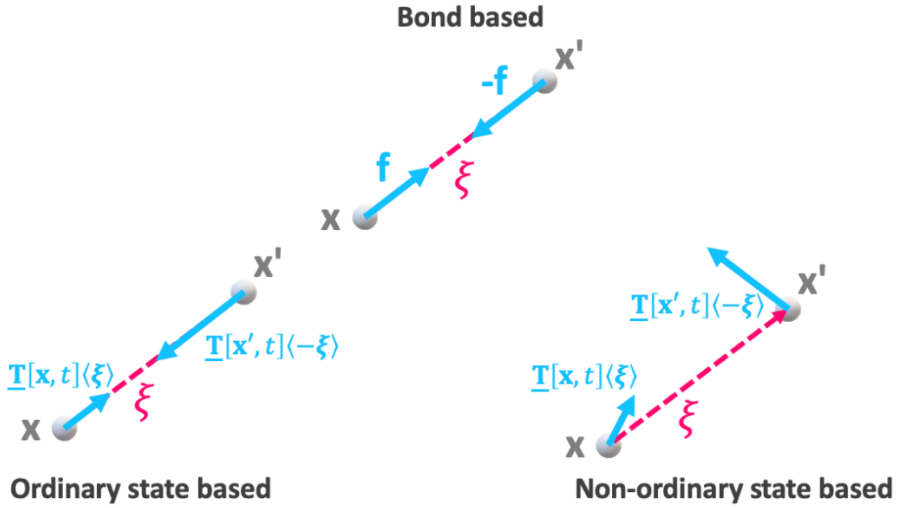

Fig. 1. Schematics of the bond based, ordinary state based and non-ordinary state based approaches.

To solve the problems of solid mechanics Eq.(4)can be discretized and the integral can be replaced with a finite sum.

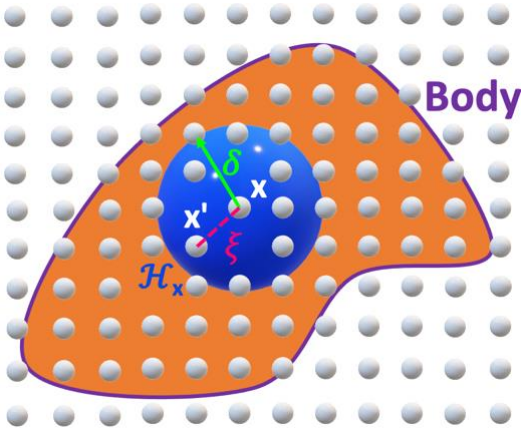

Fig. 2. Schematic of peridynamic discrete representation.

Damage of the peridynamic point is determined as the fraction of broken bonds connected to the point:

$$\varphi(\mathbf{x},t)=\frac{\int_{\mathcal{H}}\big(1-\beta(\xi,t)\big)dV_{\xi}}{\int_{\mathcal{H}}dV_{\xi}} \qquad (7),$$

$$\text{where } \beta(\boldsymbol{\xi},t)=\begin{cases}1, \text{if bond damage criterion is satisfied } \forall t'\le t\\ 0, \text{otherwise}\end{cases},$$

and this way, peridynamics is naturally suitable for simulations of the material degradation which is now studied even for very complex systems, e.g. granular materials [22,23].In order to implement the mean stress criterion and ITFC it is important to calculate the classical stress field. For this purpose, the shape tensor will be used:

$$\mathbf{K}[\mathbf{x}, t] = \int_{\mathcal{H}_x} \underline{\omega}\langle|\boldsymbol{\xi}|\rangle \boldsymbol{\xi} \otimes \boldsymbol{\xi}\, dV_{\mathbf{x}} \tag{8},$$

where $\underline{\omega}\langle|\boldsymbol{\xi}|\rangle$ is an influence function (this function is supposed to be spherically symmetric, and thus depending only on the bond length $|\boldsymbol{\xi}|$) and in the presented study both the unity and Gaussian influence functions are discussed. The unit influence function is defined as:

$$\underline{\omega}\langle|\xi|\rangle = \begin{cases} 1, \text{if} \dfrac{|\boldsymbol{\xi}|}{\delta} \le 1 \\ 0, \text{otherwise} \\ \text{or if bond is broken} \end{cases} \tag{9}.$$

The Gaussian influence function is defined as (Fig. 3):

$$\underline{\omega}\langle|\xi|\rangle = \begin{cases} e^{-\left(\frac{|\xi|}{0.4\delta}\right)^2}, \text{if} \dfrac{|\boldsymbol{\xi}|}{\delta} \le 1 \\ 0, \text{otherwise} \\ \text{or if bond is broken} \end{cases} \tag{10}.$$

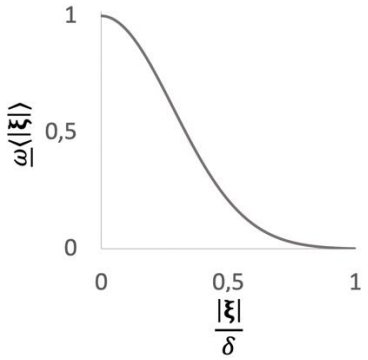

Fig. 3. Gaussian influence function.

Then, deformation gradient tensor **F** can be obtained by reduction of the deformation vector state:

$$\mathbf{F}[\mathbf{x}, t] = \left[\int_{\mathcal{H}_x} \underline{\omega}\langle|\boldsymbol{\xi}|\rangle \left(\underline{\mathbf{Y}}\langle\boldsymbol{\xi}\rangle \otimes \boldsymbol{\xi}\right) dV_{\mathbf{x}'}\right] \mathbf{K}^{-1} \tag{11}.$$

Next,a Green-Lagrange strain tensor **E**[**x**,t] is defined as:

$$\mathbf{E}[\mathbf{x}, t] = \frac{1}{2}(\mathbf{F}^{\mathrm{T}} \cdot \mathbf{F} - \mathbf{I}) \tag{12},$$

where **I** is the identity tensor. Then, using a Hook's law we can define the Piola-Kirchhoff stress tensor $\boldsymbol{\sigma}[\mathbf{x}, t]$:

$$\boldsymbol{\sigma}[\mathbf{x}, t] = \lambda\, \mathrm{tr}(\mathbf{E})\mathbf{I} + 2\mu\mathbf{E} \tag{13},$$

where $\lambda = K - \frac{2}{3}G$, $\mu = G$ are the Lame constants, K, G are bulk and shear moduli, respectively.

3. Stress based fracture criteria

3.1 Mean stress fracture criterion (Neuber-Novogilov criterion [24,25])

Let's consider a segment with length d (ad-sized area if 3D case is considered) located along X-axis subjected to normal stresses $\sigma_y(x)$. According to the considered criterion a crack along this segment will appear if the following condition holds:

$$\frac{1}{d}\int_{x}^{x+d} \sigma_y\,(x')dx' \geq \sigma_c \qquad (14).$$

An introduction of a characteristic length parameter d is a key feature of the considered criterion.This way the fracture scale level size is set: cracks smaller than d are not considered as fracture and the crack is supposed to propagate by discrete jumps due to subsequent failure of the structural blocks of size *d* starting from the crack tip [26].

If both sides of (14)are multiplied by d, the integral on the left hand side will yield force acting on a continuation of the crack (we consider a plane problem here supposing a unity sample thickness). Thus, the criterion (14)is in fact a force-based fracture condition.

The criterion (14) is consistent with the classical Irwin's fracture criterion $K_I \geq K_{IC}$if proper d value is chosen and if Sneddon's formulas for the stress field near the crack tip are recalled. Substitution of the Sneddon's expressions into (11) provides the following value for d [26]:

$$d = \frac{2}{\pi}\frac{K_{Ic}^2}{\sigma_c^2} \qquad (15).$$

Here K_{IC} is a critical quasi-static stress intensity factor (SIF) and thus *d* can be regarded as a material constant.

It should be noted that application of (11)together with numerical methods implies natural restrictions on the body mesh size in the zone of interest: the element size should be less or equal to$d$. This refers to any numerical scheme with spatial discretization including finite element method and peridynamics. This limitation may require considerable amount of computational resources as for some materials d is small leading to extremely fine meshes.

In case when the computational resources are limited a rescaling procedure can be performed and a new characteristic size $d^* = kd, k > 1$ can be introduced. Expression (15) is supposed to hold for d^* and thus the recalculated ultimate stress value $\sigma_c^* = \sigma_c/\sqrt{k}$ should be introduced, if the Irwin's criterion is supposed to remain applicable and the ultimate SIF value K_{Ic} to be unchanged. This way, in order to use larger d to obtain larger mesh size, one should use a smaller ultimate stress value. See Fig. 4 for details.

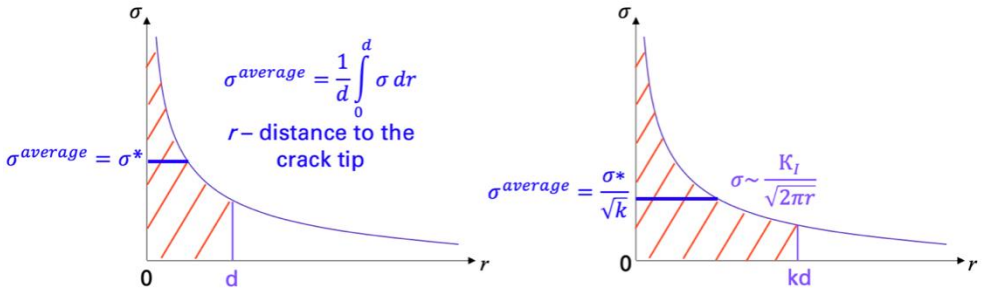

Fig. 4. Comparison of the average stress value at the crack tip vicinity on the interval of size d (on the left) and of size kd (on the right).

In fact, formula (14) is a well-known Neuber-Novohilov fracture condition introduced in, but in this particular work it is not implemented directly and thus we use a *mean stress criterion* term instead.

3.2 Incubation time fracture criterion (ITFC)

The Incubation time fracture criterion (ITFC) [6,7,26] is known as a space-time approach to dynamic fracture problems that was developed to analyse key dynamic effects of a brittle fracture. If the crack tip is currently located at a point with coordinate x on the axis along the direction of the crack, then the crack tip will move to the point with coordinate $x + d$if the following condition holds:

$$\frac{1}{\tau}\int_{t-\tau}^{t}\frac{1}{d}\int_{x}^{x+d}\sigma_y\,(x',t')dx'dt' \geq \sigma_c \qquad (16),$$

where τ is called an incubation *characteristic* time of fracture and the crack direction coincides with spatial axis in (14).The inner integral of (16) has a form of the Neuber-Novogilov static fracture criterion and thus minimal fracture surface or crack length$d$is introduced. It is also supposed that the ITFC is consistent with the classical Irwin's fracture criterion $K_I \geq K_{IC}$and thus d is selected according to formula (15).It is worth noticing that the initial interpretation of parameter d involved its connection to physical dimensions of the medium structure, e.g. grain size or interatomic distances and thus d was supposed to be used for size effects investigation which is a fruitful and important field [27]. However, the ITFC approach considers d to be a scale identifier: for the case of crack propagation d is a minimal crack increment registered within the model.

Time integration in (16) implies that fracture at the point of interest is controlled by history of the stresses rather than their current immediate values. This means that fracture is considered to be a continuous process and not an instantaneous event or in other words dynamic

fracture is “space and time non-local”. Final fracture at a chosen scale (controlled by the d parameter) is a result of preparatory processes e.g., microcracking, birth and coalescence of voids and various defects. Interestingly, such fracture process non-locality is nowadays observed experimentally in new metamaterials with complicated structures which are designed to make fracture not an instant event, but a gradual process [28,29].

These complicated processes are accounted by a single parameter – the incubation time τ, which is regarded as a material property. The incubation time τ can be obtained analytically from the experimental results on dynamic fracture [30], where stress history and fracture time are known.

The afore mentioned critical fracture condition (16) has been already effectively used to predict fracture in various problems including impact, dynamic crack propagation, spallation, solid particle erosion [30-33].

4. Implementation of the stress-based fracture criteria in peridynamics

The developed peridynamic implementation of the mean stress and incubation time approaches suppose that the bonds fail separately in the autonomous mode as it is usually considered in other fracture criteria applied in combination with the peridynamic theory. An explicit solver of the open-sourced peridynamic code Peridigm was used for numerical implementation [11].

The criterion (14) is a stress-based fracture criterion and thus, the bond failure is controlled by stresses in the elements connected by the considered bond if the ITFC is applied. As it has been mentioned earlier, the Neuber-Novogilov criterion is not implemented directly in this work and thus is referred as the mean stress fracture criterion.

Formula (14) supposes averaging of stresses over segment with length d (or over d-sized area for a 3D case) and formulas for the stress evaluation in the elements (11)-(13) map a stress tensor to the whole peridynamic element and thus these stress tensor values can be regarded as averaged over element.

Thus, if the element size is chosen to equal d, element stresses evaluated according to (11)-(13) can be used to predict a fracture. Since the bond failure is controlled by stresses, it is convenient to introduce the bond stress assuming that the bond fails if normal stress acting on some virtual area inside at least one of the considered elements exceeds some critical value, the bond fails.

This way, for the bond connecting elements A and B it is convenient to put $\sigma_{ij}^{bond} = \sigma_{ij}^{A} + \sigma_{ij}^{B}, i,j = 1..6$. In this particular case we are interested in stresses normal to the crack propagation direction which coincides with the X axis and thus it is fair to consider:

$$\sigma_y^{bond} = \sigma_y^A + \sigma_y^B \quad (17).$$

It is worth noticing that for the extreme scenario when, for example, $\sigma_y^A = \sigma_c$ and$\sigma_y^B = 0$ the bond will still fail. Formula (17) can be obviously rewritten using a more conventional expression for the bond stress [34,10] $\sigma_y^{bond} = \left(\sigma_y^A + \sigma_y^B\right)/2$, however this requires utilization of a halved ultimate stress value since we suppose that the bond should fail in the mentioned extreme case ($\sigma_y^A = \sigma_c$, $\sigma_y^B = 0$).

Since the element size is selected to be d and the stresses σ_y^A and σ_y^B are considered as mean stresses for the elements A and B, the mean stress criterion reads as:

$$\sigma_y^{bond} \geq \sigma_c \quad (18).$$

If the d parameter appears to be too small resulting in unacceptably fine mesh and a new mesh size $d^* = kd, k > 1$ has to be used, the above described rescaling procedure should be applied and the right side of (18) should be substituted by $\sigma_c/\sqrt{k}$.

$$\sigma_y^{bond} \geq \frac{\sigma_c}{\sqrt{k}} \quad (19).$$

For the ITFC the bond stress definition, the d parameter selection according to (15) and possible rescaling are also valid and the main technical difference from the mean stress criterion is time integration. Thus, the following condition should be checked if the ITFC is used for the bond failure prediction:

$$\frac{1}{\tau}\int_{t-\tau}^{t} \sigma_y^{bond} dt' \geq \sigma_c \quad (20).$$

Again, for the meshes with larger elements with size $d^* = kd, k > 1$ the right side of (20) should be changed to $\sigma_c/\sqrt{k}$. The outer temporal integral in (20) is calculated using a trapezoidal rule based on the sufficient time interval and simulation timestep should be smaller than the incubation timeτ.

5.Quasi-static verification tests

In order to test the implemented criterion quasi-static tensile tests were conducted with a pre-notched plate.The main purpose was to compare energy release rates of the running crack using the classical critical bond stretch criterion, which is analogous to the classic Griffith

criterion in peridynamic formulation. Relation of the critical stretch value in case of state-based peridynamics was taken from [14].

The energy release rate was calculated using Rice-Cherepanov J-Integral approach. The displacement-based method described in [35] was used for this purpose. The fact that in the state-based peridynamics we can calculate deformation gradient tensor **F** from the deformation state **Y**allows one to calculate J-Integral via displacement field. A stationary contour embracing sufficiently large domain was used for the J-integral calculations (Fig.5).

In these tests rectangular PMMA specimens with a size of 80 mm x 50 mm were used. In all experiments prescribed displacements are applied to the left edges with a width of two horizons (2δ) as it is shown in Fig.5.The length of the pre-notch is 15 mm and the J-Integral contour size is 60 mm x 17 mm. Relatively low crack propagation velocities (100-140 m/s) were observed in the cases discussed below.

The problem was solved in a three-dimensional configuration since Peridigm is implemented for 3D case.

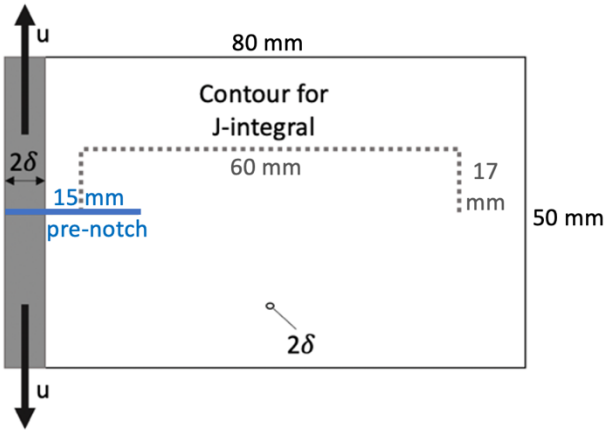

Fig.5. Conditions of the quasi-static verification tests.

Table 1. Mechanical properties of PMMA.

Density	1230 kg/m^3
Young's modulus	3.5 GPa
Poisson's ratio	0.35
Critical SIF, K_{IC}	1 MPa$\sqrt{\text{m}}$
Critical energy release rate, G_{1C}	0.286 N/mm
Ultimate tensile stress, σ_c	60 MPa
Structural block size, d	0.177 mm
Incubation time, τ	1.5 μs

In all tests presented in this papera horizon size is taken as $\delta = 3\Delta x$ as it is shown to be a numerically stable choice [36]. Specimen thickness is equal to 2δ and, thus, it is different in the presented cases. Acrack tip position is determined as the rightest element with a damage value of 0.35 or greater [36].

All the results presented below on Fig.6-Fig. 9 contain the energy release rate dependences averaged over 40 μs (upper graphs) and non-averaged dependences of the crack tip position (lower graphs).

Firstly, we studied how the classic Griffith criterion correlates to the mean stress fracture criterion. As seen from Fig.6, the energy release rate for a crack moving according to mean stress criterion is close to a static critical value G_{1c}, which can be regarded as a good indication of the mean stress criterion applicability and potential of the stress-based fracture criteria for peridynamics in general.

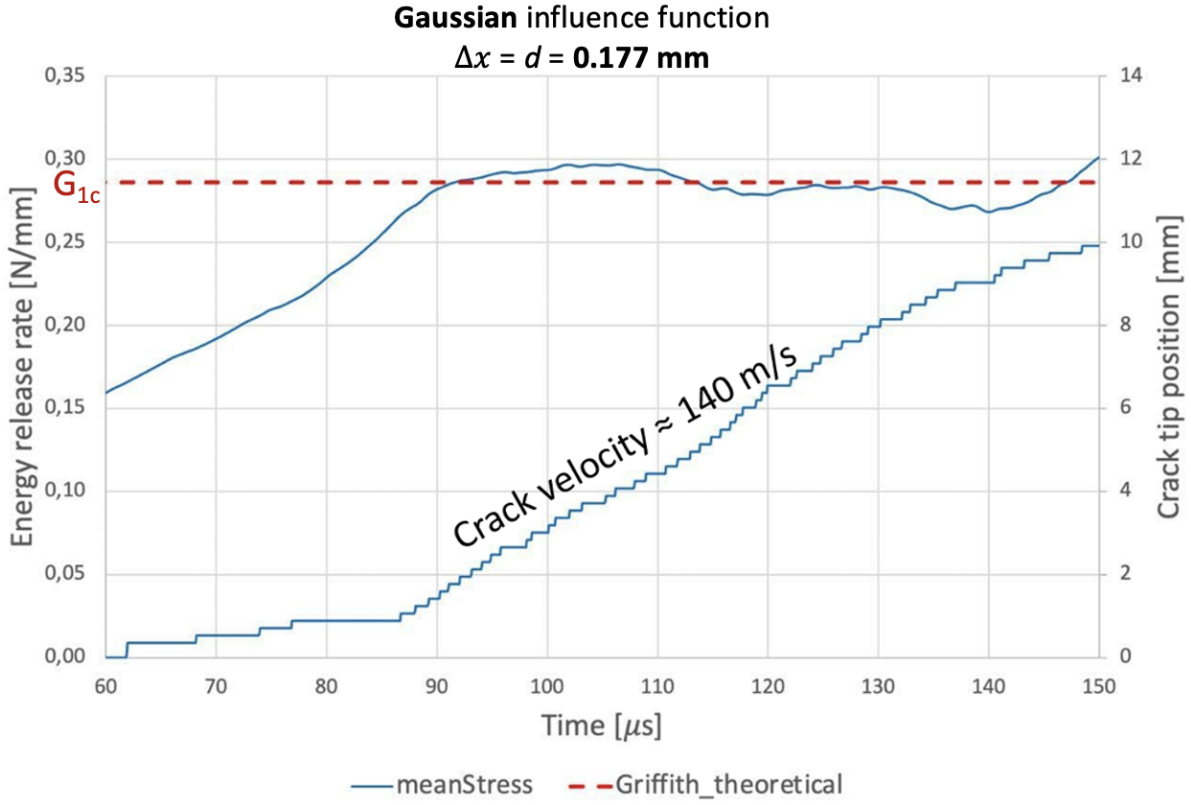

Fig.6.Comparison of the theoretical static critical value G_{1c} and mean stress criterion for $\Delta x=d$=0.177 mm in case of the Gaussian influence function.

In addition to this, we tested the mean stress criterion, the ITFC and the critical stretch criterion for three different mesh sizes in order to check how the rescaling procedure works. The minimum element size is equal to 0.177 mm – a value calculated according to formula (15).

The two other element sizes are: 0.5 mm and 1 mm. The corresponding results are shown in Fig. 7-Fig. 9, where a unit influence function was used.

As seen from Fig. 7 - Fig. 9, the energy release rates during crack propagation as well as the dependences of the crack tip position governed by the mean stress criterion are close to those governed by the classical critical bond stretch criterion for all considered element sizes. This could be seen as a good indication of the rescaling procedure applicability at least for the mean stress fracture criterion.

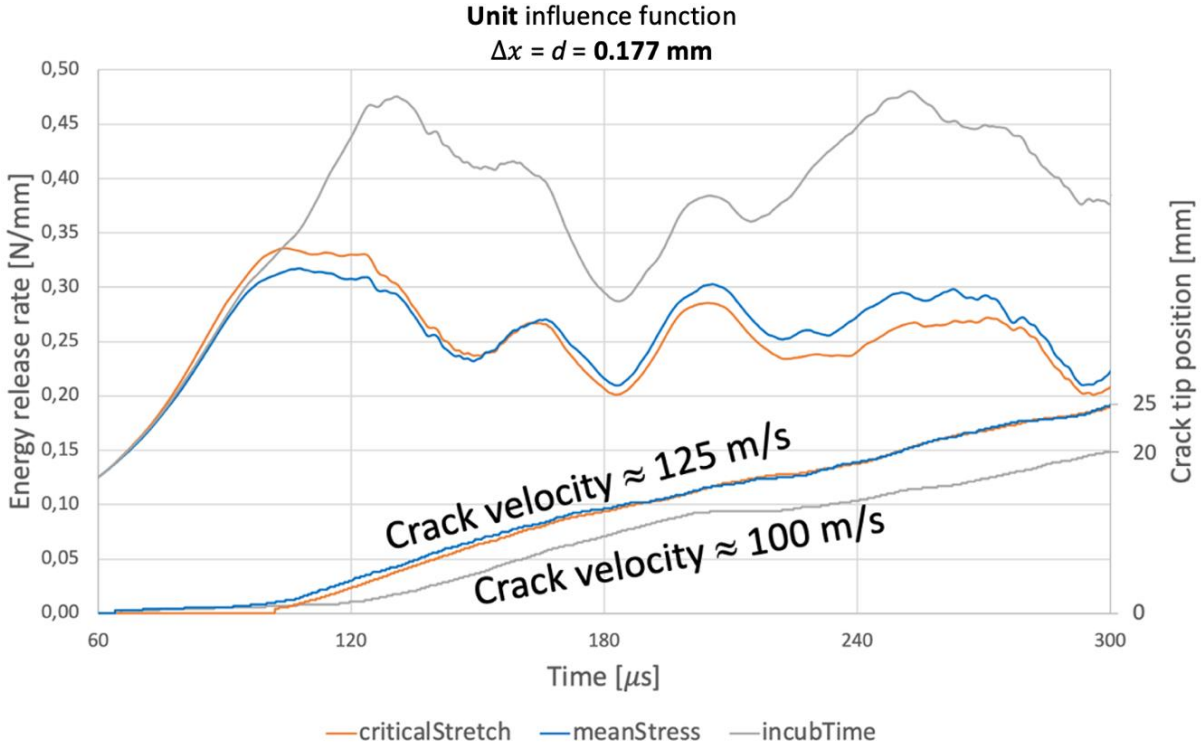

Fig. 7. Comparison of the critical stretch, mean stress and incubation time criteria for Δx=d=0.177 mm in case of the unit influence function.

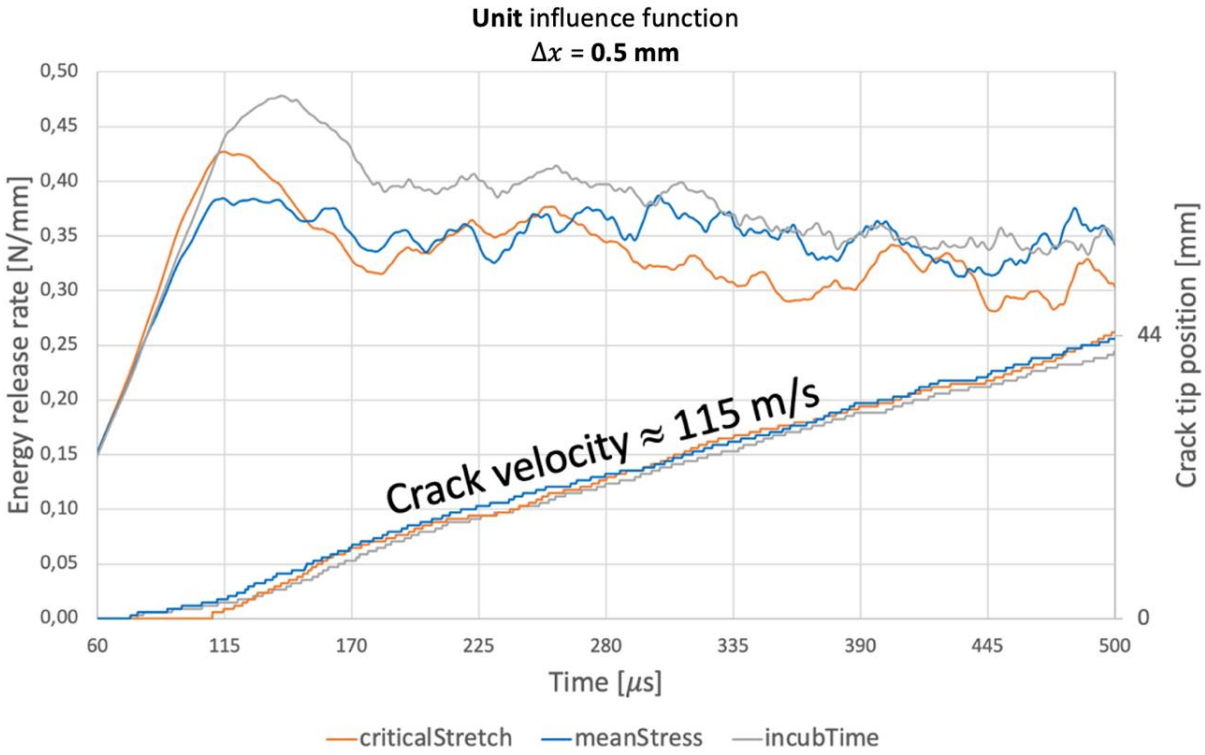

Fig.8.Comparison of the critical stretch, mean stress and incubation time criteria for Δx=0.5 mm in case of the unit influence function.

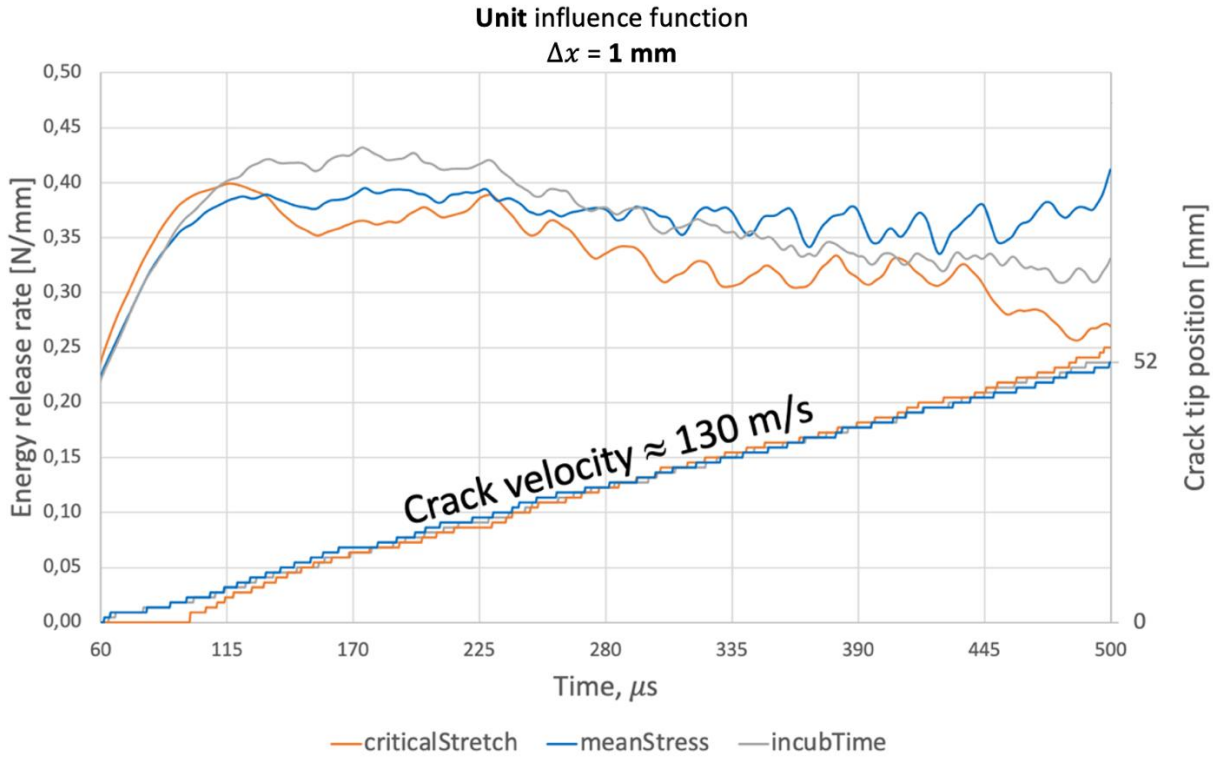

Fig. 9. Comparison of the critical stretch, mean stress and incubation time criteria for Δx=1 mm in case of the unit influence function.

In case of the $\Delta x=d$=0.177, the best correlation was observed between a mean stress and critical stretch criteria. Meanwhile, in this case, ITFC demonstrates the highest energy release rate and the lowest crack velocity, that corresponds well to both the numerical results of finite-element modelling using ITFC in [37] and experimental data [38].

All the results shown in Fig.6 - Fig. 9 are presented for different time intervals for which a relatively constant energy release rate was observed. After that, in cases presented in Fig.6 - Fig. 7, there is a divergence in the energy release rates for all presented criteria, apparently because of the peridynamic boundary effect due to incomplete horizons of boundary or near-boundary points. Additional correction algorithms could be used to address this problem [14, 39].

The latter means that elastic waves reflected multiple times from the boundaries affect the stress waves, that are especially important for the crack propagation governed by the stress-based fracture criteria presented here. Due to varying sample thicknesses, out-of-plane elastic waves could also affect the energy release rate in different ways. This could be avoided in a 2D analysis, that would also possibly improve the presented results.

It is worth noting that although both models demonstrated a generally continuous crack propagation, some short stops were observed, that explains some deviations of the measured energy release from the G_{1c}value. Obviously, the choice of the element size as well as the influence function also affects the deviation of the measured energy release from G_{1c} value. As seen from Fig.6-Fig. 9, the results obtained using the mean stress fracture criterion, ITFC and the critical bond stretch criterion are in good agreement in terms of the current energy release rate, the crack tip position and the crack velocity. It was also observed that the cracks modelled by aforementioned criteria visually look identical, i.e. thickness of the damaged elements zone, as well as the level of their damage.

6. Conclusion

The work presents peridynamic implementation and numerical testing of the stress-based fracture criteria. An explanation of the proposed modifications of the structural-time fracture criteria for use in peridynamics was given. For the test case (relatively slow crack propagation due to quasistatic load) the presented method is in good agreement with the classical Griffith theory. On the other hand, application of the incubation time fracture model allows one to investigate problems where classical criteria will possibly fail or require serious modifications, e.g. the widely used stress-intensity factor criteria perform poorly when applied to crack initiation problems due to high-rate load requiring adjustment for each particular

loading rate. The mean stress fracture criterion and ITFC does not rely on the SIF value but rather operates with stresses and thus, provides possibility to evade the mentioned problems. This way, the proposed implementation of the aforementioned criteria can possibly broaden applicability of the peridynamic theory.

Acknowledgements

This work was supported by the Russian Foundation for Basic Research (No. 19-31-60037). Sections 1 and 5 were made by Yuri Petrov within the framework of the Russian Science Foundation project (No. 22-11-00091). The authors are grateful to Mikhnovich I.V. for assistance in writing a program code.

References

[1] Griffith A. A. VI. The phenomena of rupture and flow in solids. Philosophical transactions of the royal society of London. Series A, containing papers of a mathematical or physical character, Vol. 221, No. 582-593, pp. 163-198, 1921.

[2] A. Kashtanov, Yu.V. Petrov, Fractal models in Fracture Mechanics, International Journal of Fracture, 2004, 128, 271-276.

[3] C.C. Ma, L.B. Freund, The extent of the stress intensity factor field during crack growth under dynamic loading conditions, ASME J Appl Mech 53 (1986) 303–310. https://doi.org/10.1115/1.3171756.

[4] Ravi-Chandar, K., & Knauss, W. G. (1984). An experimental investigation into dynamic fracture: III. On steady-state crack propagation and crack branching. International Journal of fracture, 26(2), 141-154

[5] J.F. Kalthoff, On some current problems in Experimental Fracture dynamics, Workshop on dynamic fracture, California Institute of Technology (1983) 11-25

[6] Y.V. Petrov, A.A. Utkin, Dependence of the dynamic strength on loading rate. Soviet Materials Science 25(2) (1989) 153–156. https://doi.org/10.1007/BF00780499

[7] Petrov, Y. V., & Morozov, N. F. (1994). On the modeling of fracture of brittle solids. J. Appl. Mech. 61:710–712.

[8] Silling, S. A., & Askari, E. (2005). A meshfree method based on the peridynamic model of solid mechanics. Computers & structures, 83(17-18), 1526-1535.

[9] Ignatiev, M. O., Petrov, Y. V., & Kazarinov, N. A. (2021). Simulation of Dynamic Crack Initiation Based on the Peridynamic Numerical Model and the Incubation Time Criterion. Technical Physics, 66(3), 422-425.

[10] Ignatev, M., Kazarinov, N., Petrov, Yu. Peridynamic modelling of the dynamic crack initiation. Procedia Structural Integrity, 28C, 1657-1661 (2020).

[11] M.L. Parks, D.J. Littlewood, J.A. Mitchell, and S.A. Silling, Peridigm Users' Guide, Tech. Report SAND2012-7800, Sandia National Laboratories, 2012.

[12] Silling, S. A. (2000). Reformulation of elasticity theory for discontinuities and long-range forces. Journal of the Mechanics and Physics of Solids, 48(1), 175-209.

[13] Silling S. A. et al. Peridynamic states and constitutive modeling //Journal of Elasticity. – 2007. – Т. 88. – №. 2. – С. 151-184.

[14] Madenci, E., & Oterkus, E. (2014). Peridynamic theory and its applications. New York: Springer.

[15] Bobaru, F., Foster, J. T., Geubelle, P. H., & Silling, S. A. (Eds.). (2016). Handbook of peridynamic modeling. CRC press.

[16] Oterkus, E., Oterkus, S., & Madenci, E. (Eds.). (2021). Peridynamic Modeling, Numerical Techniques, and Applications. Elsevier.

[17] Dell'Isola, F., Andreaus U., Placidi L. (2015). At the origins and in the vanguard of peridynamics, non-local and higher-gradient continuum mechanics: an underestimated and still topical contribution of Gabrio Piola, Mathematics and Mechanics of Solids 20.8, 887-928.

[18] Dell'Isola, F., Della Corte A., Giorgio I. (2017) Higher-gradient continua: The legacy of Piola, Mindlin, Sedov and Toupin and some future research perspectives, Mathematics and Mechanics of Solids 22.4, 852-872.

[19] Marconi V.I., Jagla E.A. (2005) Diffuse interface approach to brittle fracture, Phys. Rev. E 71 036110

[20] Randles P, Libersky L. (1997) Recent improvements in SPH modeling of hypervelocity impact. Int J Impact Eng 20, 525–32.

[21] http://www.peridynamics.org/what-is-peridynamics

[22] E. Placidi, L., Barchiesi, E., Misra, A. and Timofeev, D. (2021) Micromechanics-based elasto-plastic-damage energy formulation for strain gradient solids with granular microstructure, Continuum Mechanics and Thermodynamics, 33, 2213-2241

[23] D. Timofeev, D., Barchiesi, E., Misra, A. and Placidi, L., (2021) Hemivariational continuum approach for granular solids with damage-induced anisotropy evolution, Mathematics and Mechanics of Solids, 26(5) 738-770 (doi: 10.1177/1081286520968149)

[24] Neuber H. Kerbspannungslehre (Notch Stresses), (1937). Verlag von Julius Springer, Berlin.

[25] Novozhilov V. V. On a necessary and sufficient criterion for brittle strength: PMM vol. 33, n≗ 2, 1969, pp. 212–222. Journal of Applied Mathematics and Mechanics, Vol. 33, No. 2, pp. 201-210, 1969

[26] Petrov YV (1991) On “quantum” nature of dynamic fracture of brittle solids. Dokl Akad Nauk USSR 321:66–68.

[27] B. Maksimov, V., Barchiesi, E., Misra, A., Placidi, L., and Timofeev, D., (2021) Two-dimensional analysis of size effects in strain gradient granular solids with damage-induced anisotropy evolution, Journal of Engineering Mechanics, 04021098-1

[28] De Angelo, M., Spagnuolo, M., D'Annibale, F. et al. (2019) The macroscopic behavior of pantographic sheets depends mainly on their microstructure: experimental evidence and qualitative analysis of damage in metallic specimens. Continuum Mech. Thermodyn. 31, 1181-1203. https://doi.org/10.1007/s00161-019-00757-3

[29] dell'Isola, F., Seppecher, P., Alibert, J.J. et al., (2019). Pantographic metamaterials: an example of mathematically driven design and of its technological challenges. Continuum Mechanics and Thermodynamics, 31 (4), 851-884. (doi: 10.1007/s00161-018-0689-8

[30] A. Gruzdkov, E. Sitnikova, N. Morozov, Y. Petrov, Thermal effect in dynamic yielding and fracture of metals and alloys, Mathematics and Mechanics of Solids 14 (2009) 72-87. https://doi.org/10.1177/1081286508092603.

[31] Y.V. Petrov, B.L. Karihaloo, V.V. Bratov, A.M. Bragov, Multi-scale dynamic fracture model for quasi-brittle materials// International Journal of Engineering Science 61 (2009) 3–9. https://doi.org/10.1016/j.ijengsci.2012.06.004.

[32] V. Bratov, Y. Petrov, Application of incubation time approach to simulate dynamic crack propagation, Int. J. Fract. 146 (2007) 53-60. https://doi.org/10.1007/s10704-007-9135-9.

[33] A. Evstifeev, N. Kazarinov, Yu.V. Petrov, L. Witek, A. Bednarz, Experimental and theoretical analysis of solid particle erosion of a steel compressor blade based on incubation time concept, Engineering Failure Analysis 87 (2018) 15-21. https://doi.org/10.1016/j.engfailanal.2018.01.006.

[34] Hattori, G., Trevelyan, J., & Coombs, W. M. (2018). A non-ordinary state-based peridynamics framework for anisotropic materials. Computer Methods in Applied Mechanics and Engineering, 339, 416-442.

[35] Stenström, C., & Eriksson, K. (2019). The J-contour integral in peridynamics via displacements. International Journal of Fracture, 216(2), 173-183.

[36] Ha, Y. D., & Bobaru, F. (2010). Studies of dynamic crack propagation and crack branching with peridynamics. International Journal of Fracture, 162(1-2), 229-244

[37] Kazarinov, N., Bratov, V., & Petrov, Y. V. (2014). Simulation of dynamic crack propagation under quasistatic loading. In Applied Mechanics and Materials (Vol. 532, pp. 337-341). Trans Tech Publications Ltd.

[38] Fineberg, J., Gross, S. P., Marder, M., & Swinney, H. L. (1992). Instability in the propagation of fast cracks. Physical Review B, 45(10), 5146.

[39] Le Q. V., Bobaru F. Surface corrections for peridynamic models in elasticity and fracture //Computational Mechanics. – 2018. – Vol. 61. – №. 4. – pp. 499-518